2013 IREP Symposium-Bulk Power System Dynamics and Control –IX (IREP), August 25-30, 2013, Rethymnon, Greece

Short-Circuit Current Contribution of Converter Interfaced Wind Turbines and the Impact on System Protection

Evangelos Farantatos
Electric Power Research Institute (EPRI)

Ulas Karaagac, Hani Saad, Jean Mahseredjian
Ecole Polytechnique de Montreal

Abstract

Traditional short-circuit modeling techniques and the associated models existing in commercially available packages are not accurate enough and do not accurately represent the behavior of converter interfaced renewable energy resources during short-circuit events. To address those issues, detailed EMT-type, time domain models of Type III and Type IV wind turbines have been developed as part of this work. Those models can be used to achieve an improved understanding of the way in which these devices affect system protection and of improved short-circuit models for system studies. The potential impact of renewable energy resources on relay misoperation and protection coordination is discussed, given that depending on the type of the wind turbines and the associated controls, the short circuit current contribution of a wind park might be the same for different locations of the fault. Finally, presently available modeling techniques of renewables in frequency domain are presented and compared. Their disadvantages are discussed along with an approach for improved modeling.

Introduction

Utilities are under considerable pressure to increase the percentage of renewable energy resources in their generation fleet. The DOE has outlined a plan to increase the percentage of power generated in the U.S. from wind power to 20% by 2030, and large-scale PV integration will increase the percentage of renewable energy resources even higher. The integration of renewable energy resources into the transmission grid presents significant technical challenges for system protection and planning engineers. The power electronics associated with some wind turbine generators (WTGs) and photovoltaic (PV) inverters can produce current waveform signatures that are significantly different from those of traditional synchronous or asynchronous generators. Traditional short-circuit (SC) modeling techniques do not accurately represent the behavior of renewable energy resources during SC events and accurate SC models of renewable energy resources are not available. Consequently, protection and system planning engineers are required to make judgments based on limited information about the behavior of these devices during SC events. As the percentage of renewable energy resources increases, so will the likelihood of experiencing problems caused by the assumptions being made regarding the SC behavior of renewable energy resources.

The paper initially presents generic EMT-type time domain models of Type III and Type IV WTGs that have been developed in order to study the SC characteristics of converter interfaced WTGs. Usually, these kind of models developed by the corresponding manufacturer of the WTG are proprietary, and the details of the controls are not disclosed. The models developed in this work will contribute to achieve a better understanding of the SC current contribution of WTGs that depends on the control schemes and the internal protection systems of the WTG. Several scenarios of faults have been tested using those models, to evaluate the SC contribution of the WTGs. Based on the results, the potential impact of renewables on the protection of the system is also discussed as it was illustrated that under specific conditions, the SC current contribution of the renewables is independent on the location of the fault that could result in miscoordination of the relays. Given the understanding of the SC characteristics of converter interfaced renewables obtained by the developed EMT-type time domain models, the ultimate goal is to develop frequency domain, phasor-type, SC models that will be included in commercial SC analysis software. Towards this goal, the paper, presents the presently available and most commonly used techniques for modeling renewables in short circuit studies. An actual case of an existing solar plant is used as a testbed to present the disadvantages of those techniques. In addition, an improved modeling approach is discussed.

WTG Time Domain Models

In order to better understand and evaluate the short-circuit current contribution of converter interfaced WTGs, detailed time domain models of Type III and Type IV

978-1-4799-0199-9/13/$31.00 ©2013 IEEE

WTGs have been developed and incorporated in EMTP-RV [1]. A short description of those models follows next.

Type III – DFIG model

The typical configuration of a Type III WTG is shown in Figure 1. The stator of the doubly fed induction generator (DFIG) is directly connected to the grid and the wound rotor is connected to the grid through a back-to-back (BtB) converter system. The BtB converter system consists of two, three-phase pulse-width modulated (PWM) converters (Rotor-Side Converter (RSC) and Grid-Side Converter (GSC)) connected by a dc bus. A line inductor and an ac filter are used at the GSC to improve the power quality. A crowbar is used to protect the rotor-side converter (RSC) against over-currents and the dc capacitors against over-voltages. During crowbar ignition, the RSC is blocked and the machine consumes reactive power. Therefore, the dc resistive chopper is widely used to limit the dc voltage and avoid the crowbar ignition during ac faults.

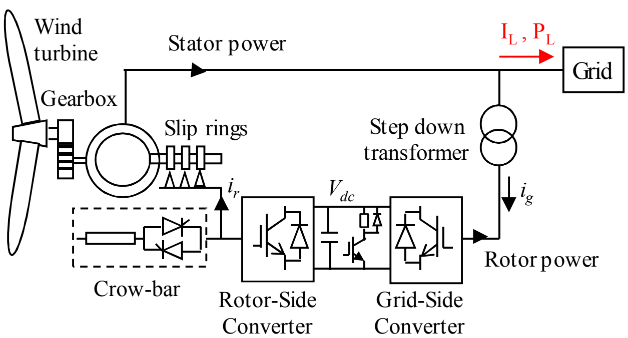

Fig. 1. DFIG Type III WTG configuration

The model implementation is based on the EMTP-RV detailed simulation time domain software [2]. The DFIG detailed model considers all the electrical components mentioned above. The wind turbine model considers a gearbox for the rotating blade and a two mass model for the mechanical shaft. The back-to-back converter is modeled using the average value model (AVM) approach [3]-[6]. The later replaces the converters power switches with equivalent controlled sources that replicate the converter behavior and decreases computational burden. The AVM accuracy has been previously verified against a detailed convertor model which replicates the nonlinear VI characteristic of power switches. It was concluded that for SC contribution studies the AVM is sufficiently accurate; however it does not represent converter harmonics.
The control of the DFIG is achieved by controlling the RSC and GSC through vector control techniques. Vector control allows decoupled control of both real and reactive powers. The RSC controls the active power delivered to the grid and ac voltage, and follows a tracking characteristic to adjust the generator speed for optimal power generation depending on wind speed. On the other hand, the GSC is used to maintain the dc bus voltage and to support the grid with reactive power during faults. Details on DFIG wind turbines control are given in [7].
The aggregated model of a 1.5 MW, 60 Hz DFIG wind turbine [3] is used in this paper. The model includes both a dc resistive chopper and a crowbar. It should be noted that, the crowbar provides backup protection to the dc resistive chopper and does not operate unless the dc resistive chopper is deactivated.
The simplified control diagram of the DFIG model is shown in Fig. 2. In addition to the dc resistive chopper and crowbar controls, the protection system block in Fig. 2 includes:

- low voltage and overvoltage relays,
- an overcurrent protection for GSC and RSC which temporary blocks the converter that is subjected to overcurrent,
- a deep voltage sag detector which temporary blocks the GSC and RSC in order to restrict the fault ride-through (FRT) operation to the faults that occur outside the wind park.

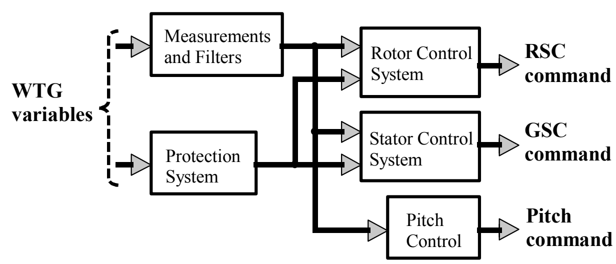

Fig. 2. Control and protection system

Type IV- FFC model

The Type IV, i.e. the full-frequency converter (FFC) WTG concept uses a permanent–magnet synchronous generator (PMSG) connected to the grid through a BtB link. Depending on the size of the wind turbine, the PMSG side converter (MSC) can be either a diode rectifier or a voltage-sourced converter (VSC). On the other hand, the GSC is typically a VSC. The BtB VSC topology is considered in this paper and shown in Fig. 3.
Similar to the DFIG, the detailed EMTP model of the FFC represents also all circuit components and its control system. The control of the FFC is achieved by controlling the MSC and GSC using vector control techniques [7]. The MSC controls the active power delivered by the PMSG, and follows a tracking characteristic to adjust the PMSG speed for optimal power generation depending on wind speed. The function of GSC is maintaining the dc bus voltage, i.e. transmitting the active power delivered to

the dc link by the MSC. It is also used to control the ac voltage and reactive power delivered to the grid.

A generic 2 MW, 60 Hz FFC model is used in studies of this paper. The model includes a pitch control, a dc resistive chopper, low voltage and overvoltage relays. A two-mass model is used to represent the turbine drive system. The FFC converters are modeled with their AVMs.

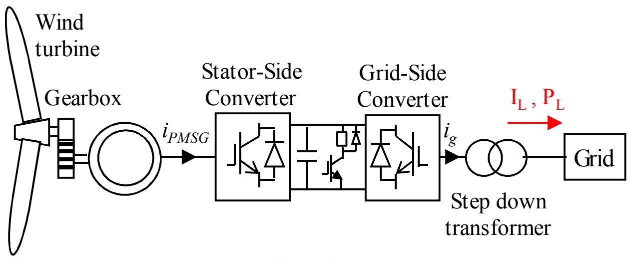

Fig. 3. FFC Type IV WTG configuration

WTG Frequency Domain SC Models

Despite the fact that the developed, detailed, time domain models can simulate accurately the SC current contribution of converter interfaced WTGs, it is uncommon for protection engineers to use them for protection studies, since frequency domain short-circuit packages are mostly used. As a result, frequency domain models have to be developed and eventually integrated in commercially available short-circuit analysis software by vendors for use in protection studies, relay coordination, and wide area coordination simulations. Improved sequence models for Type I WTGs have been developed in [8]-[9]. Those models though, cannot be used for modeling Type III and Type IV WTGs due to the converter interface to the grid which changes their short circuit behavior.

Presently in the utilities' short circuit databases, renewables are usually modeled as a classical synchronous generator model using a voltage source behind an impedance. However, the SCC contribution of the converter interfaced renewables is limited by the power converter and depends on the control schemes of the WTG. As a result, synchronous generator models are not accurate. In most of the commercial packages, a current limiting option is also available, in which Type III and Type IV WTGs are modeled as a constant current source, independent on the terminal voltage of the WTG. The current limit is a user defined option. Although, this modeling approach is better than a synchronous generator model, it is not accurate enough to model the dependency of the fault current on the different control schemes of the WTG and the dependency of the fault current on the severity of the fault.

Upon a fault the active/reactive current contribution of the WTG is mainly imposed by the LVRT scheme that the WTGs are required to achieve in each country. The FERC Order 661 LVRT characteristic is shown in Fig. 4.

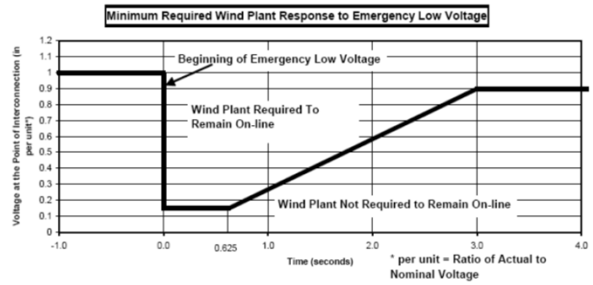

Fig. 4. US-FERC LVRT characteristic

For example a simplified reactive current control strategy is shown in Fig. 5. It is observed that the SC current depends on the severity of the fault and the voltage deep at the terminal of the renewable. As a result a more accurate modeling approach of converter interfaced renewables in frequency domain short circuit analysis, would be a voltage dependent current source, as a function of the MV WTG terminal bus voltage, as was originally suggested in [10].

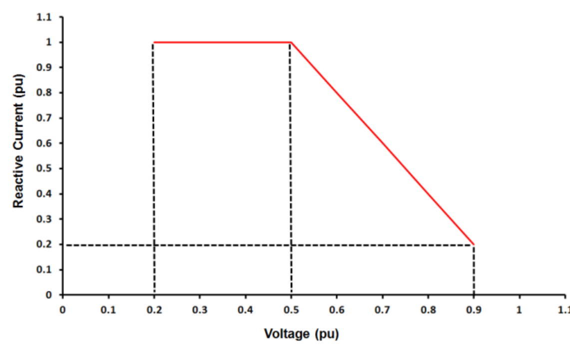

Fig. 5. Typical reactive current control curve for grid support during faults

The reference active/reactive current curves can be obtained based on WTG vendor short-circuit data or EMTP type analysis.

Demonstrating Examples

Detailed Simulation of WTG System

The EMTP-RV single line diagram of the simulated 500 kV, 60 Hz three bus system is shown in Fig. 6, along with the related load-flow data. The synchronous machine subnetwork (SM in Fig. 6) contains a detailed machine model with controls (governor and exciter) and a step-up transformer. The loads are represented by equivalent impedances connected from bus to ground on each phase. The transmission lines are represented by distributed constant parameter models. The wind farm connected to BUS2 consists of two identical stacks as shown in Fig. 7 and each stack contains an aggregated model of WTGs. The equivalent parameters for the 34.5kV equivalent collector grid are calculated on the basis of active and reactive power losses in the feeder for the rated current flow from each of the WTGs [7]. The objective of time domain simulations is to show different behaviors between type III, type IV and a synchronous machine (SM). The WTGs were assumed to operate in voltage control mode. In the simulations conducted in this paper, the following three scenarios are considered for generation connected to BUS2 (Fig. 7):

1. 90 type III WTGs (Installed capacity = 2 x 45 x 1.5 MW),
2. 68 type VI WTGs (Installed capacity = 2 x 34 x 2 MW),
3. The wind farm is replaced with a 160 MVA/135 MW single unit hydraulic power plant (HPP). The HPP model contains a detailed machine model with controls (governor and exciter) and a step-up transformer.

The simulations contain two different fault scenarios: a) a three-phase fault at BUS2 (close bus fault) and b) a three-phase fault at L3 (remote bus fault). In this paper, the short circuit behavior of the type III and type IV WTGs is of interest. In the simulations, the fault is applied at 1s and the system is simulated for 1.15s. The faults in a 500kV transmission network are expected to be cleared in less than 150ms even with the delayed operation of the protection system due a failure in one of the protective devices such as stuck circuit breaker. The simulation scenarios are summarized in Table 1.

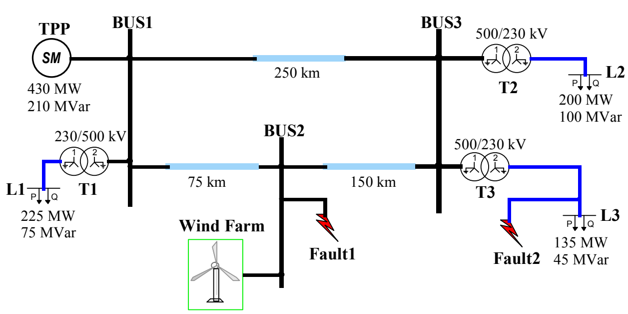

Fig. 6. EMTP-RV single line diagram of the simulated system

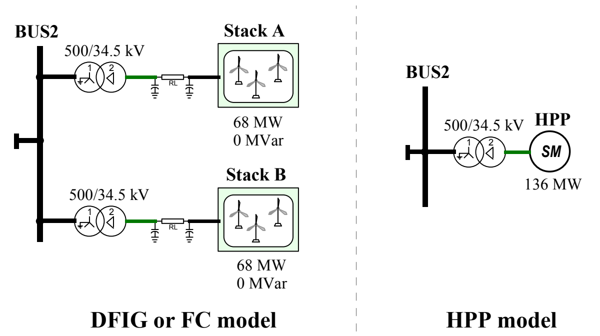

Fig. 7. Three study scenarios

Table 1. Studied scenarios

Scenario	**Generation at BUS2**	**Fault**
S1	Type-III WTG	Close bus fault
S2	Type IV WTG	Close bus fault
S3	HPP	Close bus fault
S4	Type-III WTG	Remote bus fault
S5	Type IV WTG	Remote bus fault
S6	HPP	Remote bus fault

Scenario - S1 (Type III WTG, close bus fault)

The wind farm output currents and the wind farm output powers are shown in Fig. 8, and Fig. 9, respectively. The presence of dc resistive chopper limits the dc voltage and prevents the crowbar ignition. As seen from Fig. 9, the active power output of the wind farm reduces to zero as the fault takes place at the common coupling point. Both Fig. 8 and Fig. 9 confirm that the wind farm remains connected to the grid during fault and supplies reactive currents to the grid.

The high dc component of the SC current (see Fig. 8) is mainly resulting from the sudden voltage change at IG terminals and its decay rate changes with the control parameters of DFIG converters.

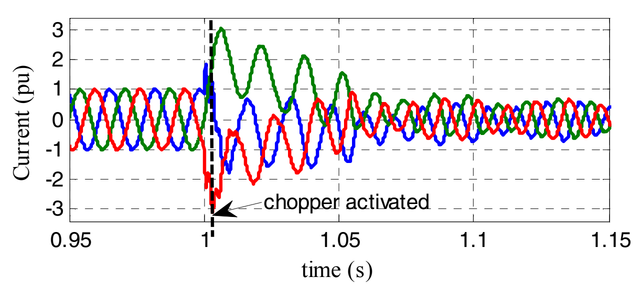

Fig. 8. Type III wind farm output currents in Scenario - S1

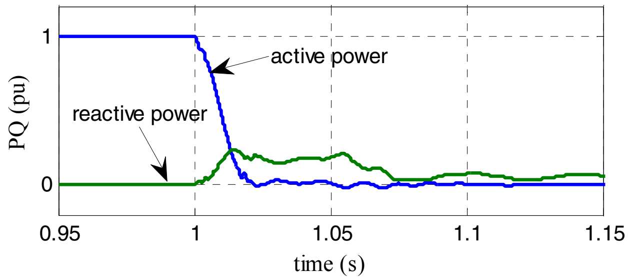

Fig. 9. Type III wind farm output powers in Scenario - S1

Scenario-S1 is repeated by deactivating the dc resistive chopper to consider the ignition of the crowbar in case of a failure in dc chopper protection. It should be also noted that some DFIG systems do not include dc resistive chopper. Fig. 10 and Fig. 11 show the current and power outputs of the DFIG without the chopper. Following the fault, the crowbar protection operates due to the rapid increase of the dc voltage. The converters are blocked and the DFIG system becomes a squirrel cage IG. However, as seen from Fig. 8 and Fig. 10, the maximum peak value of the current is less than 3.2pu in both configurations.

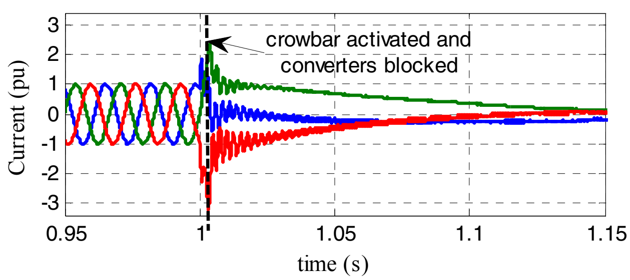

Fig. 10. Type III wind farm output currents in Scenario - S1 (without dc resistive chopper)

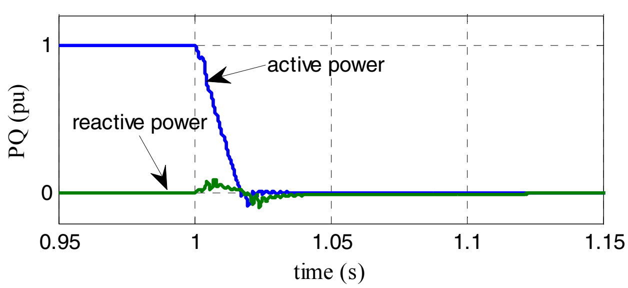

Fig. 11. Type III wind farm output powers in Scenario - S1 (without dc resistive chopper)

Scenario - S2 (Type IV WTG, close bus fault)

The current and power outputs of the FFC wind farm are shown in Fig. 12 and Fig. 13, respectively. In this WTG configuration, since only the converter side (GSC) is connected to the grid, the power electronic circuits and the associated controls affect the SC contribution. Thus, the dynamic behavior of the SC response of the WTG is much faster. Immediately after the fault, the maximum value of the current is estimated at 2.2pu and after 1 cycle it decreases to 1.27pu. Moreover, it is able to supply more reactive currents to the grid as seen from Fig. 12 and Fig. 13.

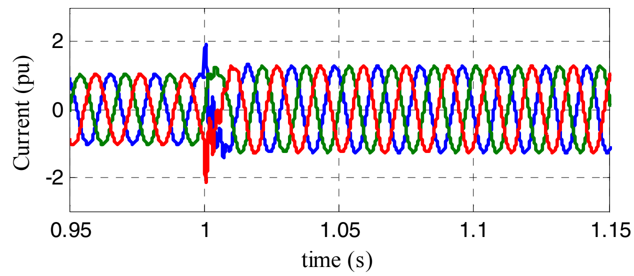

Fig. 12: Type IV wind farm output currents in Scenario-2

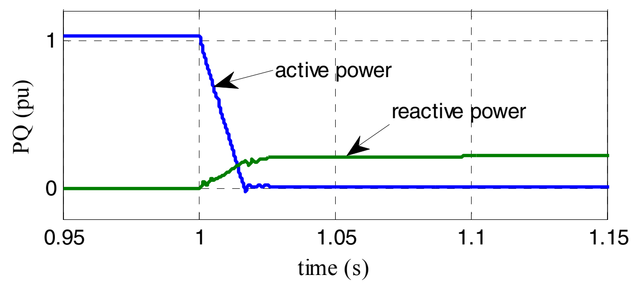

Fig. 13. Type IV wind farm output powers in Scenario-2

Scenario – S3 (HPP, close bus fault)

In this scenario the wind farm is replaced with a similar size synchronous machine with the associated controls. The current and power contributions are presented in Fig. 14 and Fig. 15 respectively. As expected, the SC contribution of the hydraulic unit is much higher compared to both type III and type IV WTGs. The maximum current reaches 10pu and the reactive power is much higher and reaches a maximum value of 1.34pu. It should be emphasized that the SC current contributions of type III and type IV WTGs are limited by their controllers.

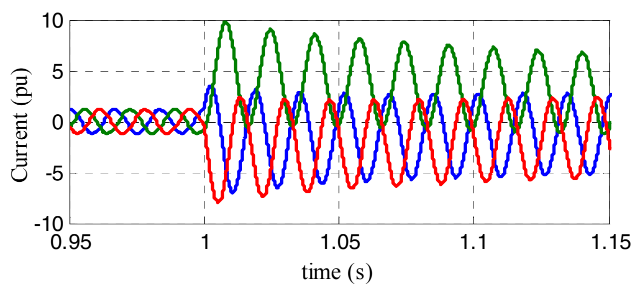

Fig. 14. HPP output currents in Scenario-3

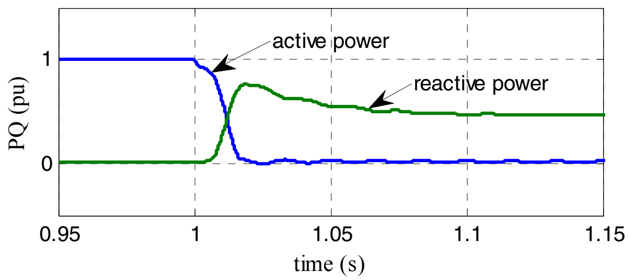

Fig. 15. HPP output powers in Scenario-3

The SC current contribution of the TPP located at BUS1 is identical in Scenarios S1 to S3 as expected and it is shown in Fig. 16.

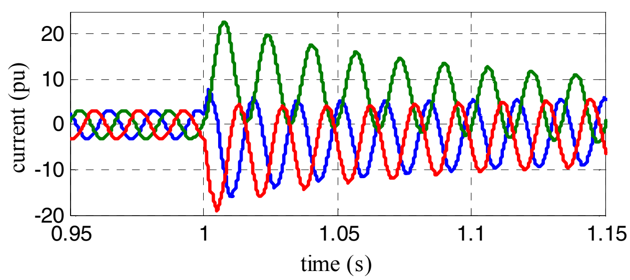

Fig. 16. TPP current output in close bus fault scenarios- S1 to S3

Scenario – S4 (Type III WTG, remote bus fault)

The current and power outputs of the DFIG wind farm are shown in Fig. 17 and Fig. 18, respectively. As seen from Fig. 17, the dc component of the SC current is much smaller and it decays much faster compared to close bus case as expected. The maximum peak value of the SC current is 1.87pu and reaches its steady-state value 1.26pu in a few cycles. Fig. 18 confirms that the wind farms supply reactive currents to the grid during fault.

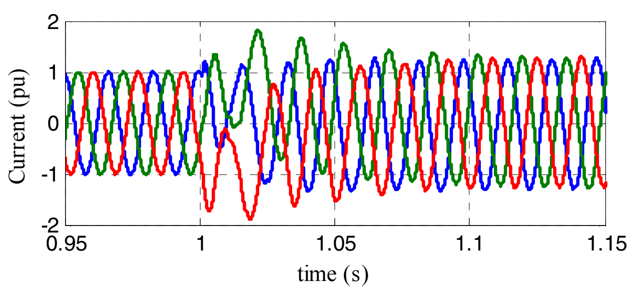

Fig. 17. Type III wind farm output currents in Scenario - S4

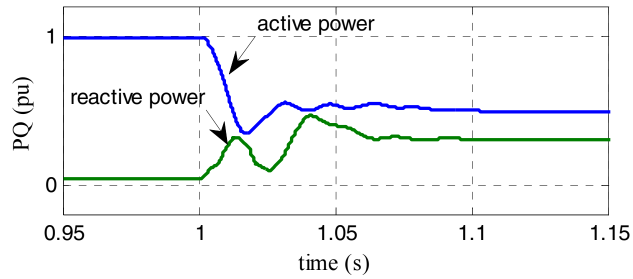

Fig. 18. Type III wind farm output powers in Scenario - S4

Scenario-S4 is repeated by deactivating the dc resistive chopper. The current and power outputs of the DFIG wind farm are shown in Fig. 19 and Fig. 20, respectively. The operation of crowbar protection turns the DFIG system into a squirrel cage IG and the wind farms start consuming reactive power. As seen from Fig. 19 and Fig. 20, active power transfer to the grid and SC current contributions are lowered as compared to the case with dc resistive chopper. The voltage waveforms at BUS2 are shown in Fig. 21and Fig. 22, for the cases with and without dc resistive chopper, respectively. Those figures demonstrate that voltage sag at BUS2 during fault becomes deeper when the DFIG does not contain the dc resistive chopper protection. The BUS 2 voltage decreases to 0.40 pu and 0.38 pu during fault for the cases with and without dc resistive chopper, respectively.

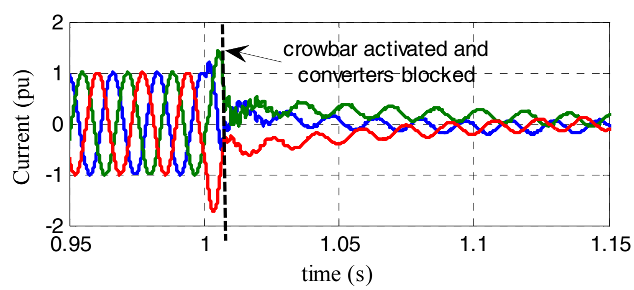

Fig. 19. Type III wind farm output currents in Scenario - S4 (without chopper)

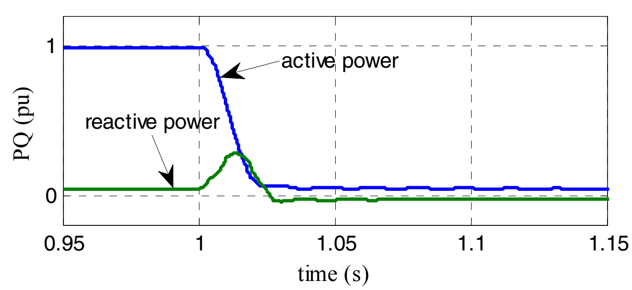

Fig. 20. Type III wind farm output powers in Scenario - S4 (without chopper)

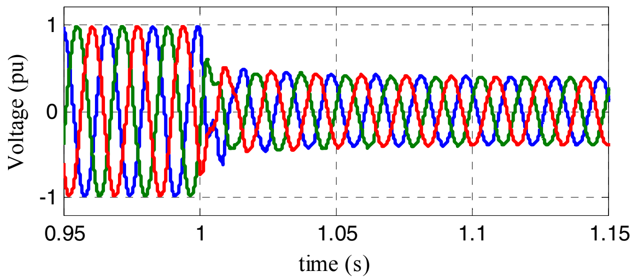

Fig. 21. BUS2 voltage waveform in Scenario - S4

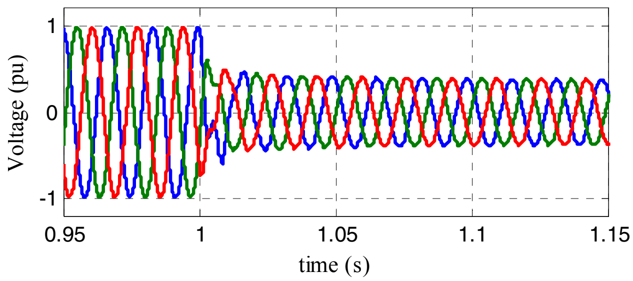

Fig. 22. BUS2 voltage waveform in Scenario - S4 (without chopper)

Scenario – S5 (Type IV WTG, remote bus fault)

The current and power outputs of the FFC wind farm are shown in Fig. 23 and Fig. 24, respectively. For the remote fault, similar short circuit response to the DFIG can be noticed. Immediately after the fault, the maximum current peak value is 1.48 pu and after 1 cycle the SC current is 1.28 pu. Reactive power is generated during the fault to support the grid.

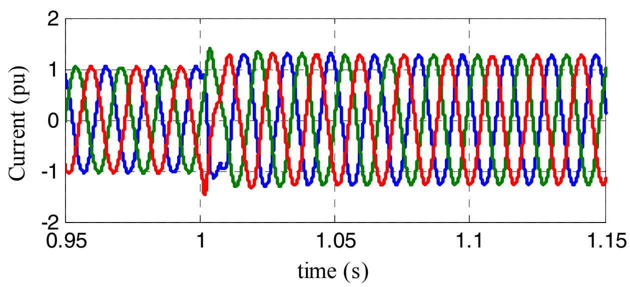

Fig. 23. Type IV wind farm output currents in Scenario – S5

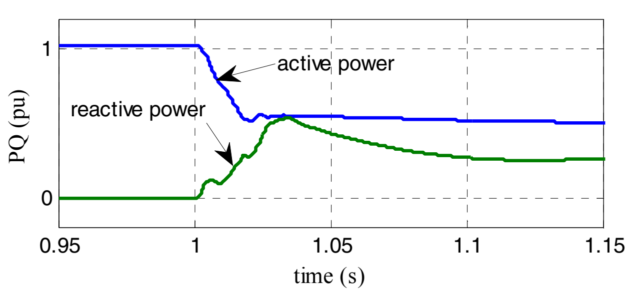

Fig. 24. Type IV wind farm output powers in Scenario – S5

In Fig. 25 the voltage waveforms at BUS2 are presented. The BUS2 voltage decreases to 0.41pu during fault.

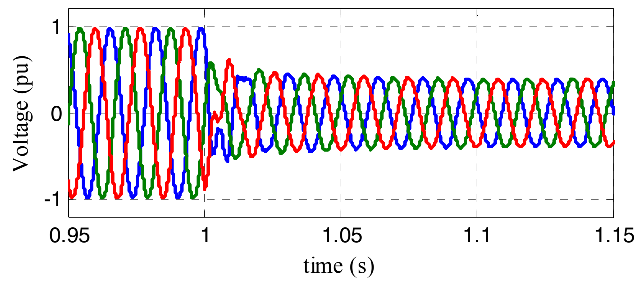

Fig. 25. BUS2 voltage waveform in Scenario – S5

Scenario – S6 (HPP, remote bus fault)

The current and power outputs of the HPP are shown in Fig. 26 and Fig. 27, respectively. The voltage waveforms at BUS2 are presented in Fig. 28 As seen from those figures the SC current contribution of HPP is much higher and the voltage support provided by the HPP is much better compared to both DFIG and FFC WTGs. The BUS2 voltage decreases to 0.48 pu during fault (Fig. 28).

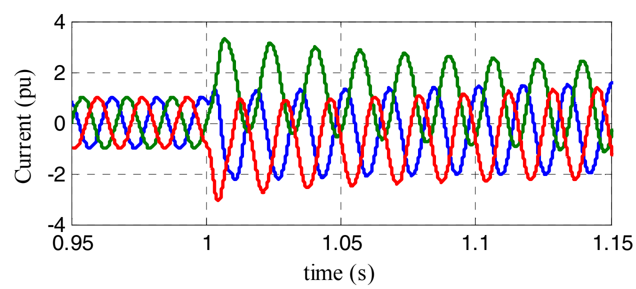

Fig. 26. HPP output currents in Scenario-S6

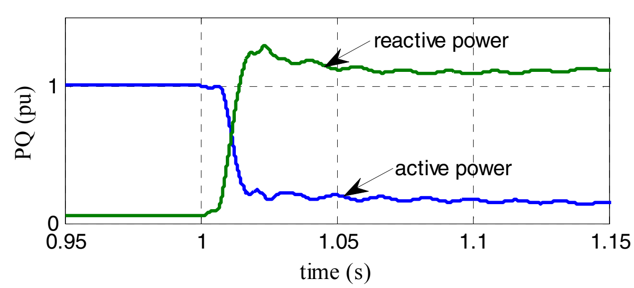

Fig. 27. HPP output powers in Scenario-S6

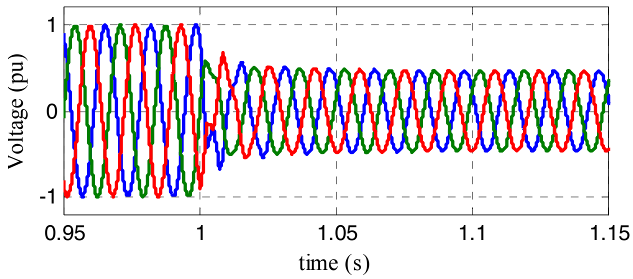

Fig. 28. BUS2 voltage waveform in Scenario - S6

The SC contribution of the TPP in Scenario-4 is presented in Fig. 29. The differences in SC contributions of the TPP are not noticiable in Scenarios S4 to S6 although the voltage profile of the system is affected significantly from the type of the power plant connected to BUS2. On the other hand, a simple three bus system is considered in this paper. The impacts of different types of power plants are expected to become more noticiable on the SC contribution of the neighbouring power plants in a larger system due to their influence on system voltage profile during faults.

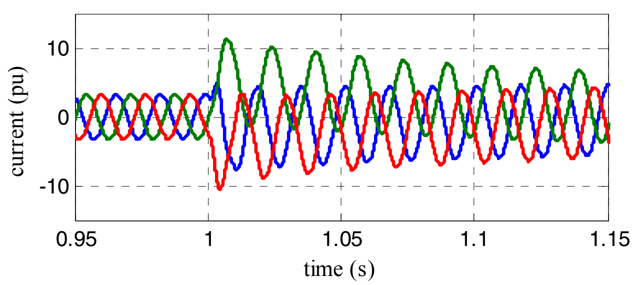

Fig. 29. Current output of the TPP in close bus fault scenarios S4 to S6

Impact of Renewables on System Protection - Discussion

The unconventional SC current waveforms that converter interfaced WTGs introduce to the grid, as was shown in the simulations before, may have a significant impact on relays performance and relays setting techniques. The constant, low value (close to nominal) fault current may result in misoperation of overcurrent or distance relays, especially in systems with increased renewables integration. In addition, a significant impact is also expected in performing protection coordination and circuit breaker duty studies.

Based on the simulation results presented before, it is concluded that the SC response of the WTG depends highly on its control scheme. For the type III WTG, the location of the fault has an impact on the SC current contribution. In case of a close fault that leads to a significant drop of the voltage at the terminal of the WTG, a SC with peak value of 3.2 pu is injected and then it decays. For a remote fault the maximum current immediately after the fault is 1.87pu and the WTG remains connected providing reactive power support to the grid.

For type IV WTG, the location of the fault does not impact considerably the SC response of the WTG. The maximum SC current is 2.2 pu for a severe fault and 1.48 pu for a remote fault. However independently of the fault location, after 1 cycle the SC contribution is the same and approximately 1.28 pu. For example, a protection coordination issue may result from the fact that the SCC of Type IV WTGs might be the same for several locations of a fault.

Comparison of Existing Frequency Domain Renewables Modeling Techniques

As was discussed before, the most common techniques that are used presently to model renewables in short circuit databases, are a classical synchronous generator model or a limited current constant source. In order to compare the results between those different modeling techniques of renewables, illustrate the different results in short circuit calculations that they yield and their disadvantages, simulations using a commercial short circuit analysis package were performed. The short circuit database of an actual system in the US was used and the focus was on an existing 125 MW solar plant. The solar plant is connected through a 5.5 miles line to the collector substation and then through a 1 miles line to a 525 kV substation, as illustrated in Fig. 27. In particular, the solar plant was modeled as a synchronous generator, a limited current source of 1.6 pu and a limited current source of 2.0 pu, for a close and distant three-phase fault with respect to the solar plant. The results are presented in Tables 2 and 3. The calculated SC current (SCC) is the current at the 525 kV line that connects the solar plant with the 525 kV bus of the corresponding substation.

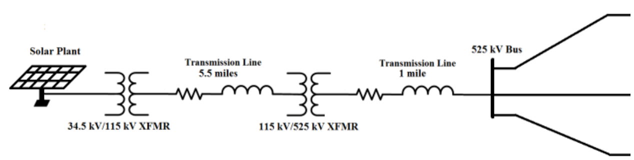

Fig. 30. Solar plant single line diagram

Table. 2. Solar plant SC analysis results - close fault

	SCC (kA)	**Solar Plant Terminal Voltage (pu)**
Synchronous Generator	0.378	0.62
Limited Current: 1.6 pu	0.224	0.37
Limited Current: 2.0 pu	0.28	0.46

Table. 3. Solar plant SC analysis results - remote fault

	SCC (kA)	Solar Plant Terminal Voltage (pu)
Synchronous Generator	0.25	0.75
Limited Current: 1.6 pu	0.224	0.57
Limited Current: 2.0 pu	0.28	0.8

It is observed that for a close fault, modeling the solar plant as a synchronous generator overestimates the SCC and the voltage at the terminal of the solar plant drops to 0.62 pu. When the solar plant is modeled as a limited current source, it is observed that for both cases (close and distant fault) the SCC is the same independently on the voltage at the terminal of the solar plant. For example, in the case of a 2.0 pu current source, the SCC is evaluated to be 0.28 kA, with the voltage being 0.46 pu for the close fault and 0.8 pu for the distant fault. As was discussed in the previous section, the SCC depends on the voltage at the terminal of the renewable so there is an inaccuracy in these computations.

Conclusions

In this paper, the unconventional short circuit current contribution of converter interfaced renewables and the potential impact on the protection of the system are addressed. EMT-type, time domain models of Type III and Type IV WTGs have been developed and presented in details. These models were used in order to evaluate and understand the short circuit characteristics of those renewables depending on the control schemes and the internal protection systems. Next, different modeling techniques of renewables in frequency domain, presently used in the industry, were compared through an actual test system of a solar plant in the US. The results indicate that there is significant difference in the short circuit current calculation depending on the modeling of the renewable. Finally, the disadvantages of those models along with a more accurate modeling technique are discussed.

References

[1] http://www.emtp.com/.

[2] J. Mahseredjian, S. Dennetière, L. Dubé, B. Khodabakhchian and L. Gérin-Lajoie: "On a New Approach for the Simulation of Transients in Power Systems". Electric Power Systems Research, vol. 77, issue 11, September 2007, pp. 1514-1520.

[3] J. Peralta, H. Saad, U. Karaagac, J. Mahseredjian, S. Dennetière and X. Legrand, "Dynamic Modeling of MMC-based MTDC Systems for the Integration of Offshore Wind Generation," CIGRE Canada Conference on Power Systems, Montreal, Quebec, Canada, September 24-26, 2012.

[4] J. Morren, S. W. H. de Haan, P. Bauer, J. Pierik, and J. Bozelie, "Comparison of Complete and Reduced Models of a Wind Turbine with Doubly-fed Induction Generator," in Proc. 10th European Conference on Power Electronics and Applications., Toulouse, France, September 2-4, 2003, pp. 1–10.

[5] J. G. Slootweg, H. Polinder, and W. L. Kling, "Representing Wind Turbine Electrical Generating Systems in Fundamental Frequency Simulations," IEEE Transactions on Energy Conversion., Vol. 18, No. 4, December 2003, pp. 516–524.

[6] U. Karaagac, H. Saad, J. Mahseredjian, S. Jensen and L. Cai, "Off-Shore Wind Power Plant Modeling Precision and Efficiency in Electromagnetic Transient Simulation Programs," in 11*th* International Workshop on Large-Scale Integration of Wind Power into Power Systems, Lisbon, Portugal, November 13-15, 2012.

[7] O. Anaya-Lara, N. Jenkins, J. Ekanayake, P. Cartwright, and M. Hughes, *Wind Energy Generation: Modelling and Control*, Wiley, 2009, John Wiley & Sons, Ltd.

[8] D.F. Howard, T.G. Habetler, R.G. Harley, "Improved Sequence Network Model of Wind Turbine Generators for Short-Circuit Studies", IEEE Transactions on Energy Conversion., Vol. 27, No. 4, 2012, pp. 968–977.

[9] D.F. Howard, T.M. Smith, M. Starke, R.G Harley, "Short circuit analysis of induction machines - wind power application", in Proc. 2012 IEEE PES Transmission and Distribution Conference and Exposition (T&D), May 7-10, 2012.

[10] R. A. Walling, E. Gursoy, B. English, "Current Contributions from Type 3 and Type 4 Wind Turbine Generators During Faults", *2011 PES General Meeting*, Detroit, MI, July 24-29, 2011.

[11] E. Muljadi, C.P. Butterfield, a Ellis, J. Mechenbier, J. Hochheimer, R. Young, N. Miller, R. Delmerico, R. Zavadil, and J.C. Smith, "Equivalencing the collector system of a large wind power plant," *2006 IEEE Power Engineering Society General Meeting*, 2006.

[12] J. M. Garcia, "Fault Current Signatures of DFIG Wind Turbines", *Texas A&M Protective Relaying Conference,* April 1, 2009.

[13] M. Reichard, "Fault Current Contributions From Variable Speed (Type 3 and 4) Wind Turbine Generators", *Texas A&M Protective Relaying Conference,* April 1, 2009.

[14] V. Gevorgian and E. Muljadi, "Short Circuit Current Contribution for Different Wind Turbine Generator Types", *Proceedings of the IEEE-PES General Meeting,* Minneapolis, MN, July 25-29, 2010.

[15] P. T. Krein, J. Bentsman, R. M. Bass, and B. L. Lesieutre, "On the use of averaging for the analysis of power electronic systems," *IEEE Trans. Power Electronics*, vol. 5, pp. 182-190, April 1990.